

Assessments

Renato Quagliani

June 15, 2015

1 OVERVIEW OF WORK DONE

A description of the work done during the first part of my PhD will be described in this document. It consists of two major blocks. The first one covers the physics analysis work that has been performed between June 2014 and October 2014. The second part of the document describes the work done in the context of the preparation for the upgrade of the LHCb detector. I worked on the improvement of a tracking as well as the development of a new algorithm: the *Hybrid Seeding*. Before getting to the heart of the work, an introduction about the tracking and the upgrade of the LHCb detector is mandatory.

1.1 INTRODUCTION TO LHCb AND TO THE UPGRADE SCINTILLATING FIBRE TRACKER (SciFi).

The aim of the LHCb detector [1] is to search for indirect signatures of New Physics through quantum loop induced processes through the measurements of strongly suppressed Standard Model processes. In this context precision plays a fundamental role.

Up to now, in LHCb and other LHC experiments, no strong deviations from the Standard Model (SM) have been observed and even if LHCb has already provided the world's best measurements in many channels, it is still limited from improving them by statistics rather than systematics. The integrated luminosity during 2011 and 2012 is 3 fb^{-1} and the expected one for the upgrade is at least 50 fb^{-2} .

For example, some measurements like the γ of the CKM matrix is still limited by statistics while lifetime measurements are already systematically limited. Due to this, the upgrade of the LHCb forward spectrometer is mandatory in order to collect $O(100)$ times more data and reduce the statistical uncertainty by a factor 10 in order to be comparable with the theoretical one [2] [3]. On top of the measurements of CP violating processes and the measurement of γ angle of the CKM matrix, the huge amount of collected data expected for the upgrade at $\sqrt{s} = 14 \text{ TeV}$ ($\sim 5 \text{ fb}^{-1}$ per year) will also strongly improve our actual knowledges about QCD and the dynamic of b and c hadrons decays.

A detailed description of the physics plan for the upgrade can be found in [2]

The LHCb detector is a single-arm forward spectrometer aiming to detect particles and their decay products, and as the b in the name of the detector suggests, it is designed to study particles containing b and c quarks which are produced strongly boosted in the forward direction (and equally the backward direction) for symmetric energies of colliding protons at $\sqrt{s}=14 \text{ TeV}$. The detailed description of the LHCb detector can be found in [1]. The data taking at LHCb during 2011 ($\sqrt{s}=7 \text{ TeV}$) and 2012 ($\sqrt{s}=8 \text{ TeV}$) is mainly determined by the trigger and the luminosity:

- Interesting events are selected by the *L0 Trigger* which is implemented at the hardware level aiming to reduce the 40 MHz bunch crossing rate to 1 MHz making use of estimations and measurements of the signature of particles having high E_T , p_T through the muon stations and the calorimeters. The main reason why this is done is because the read-out system of some of the detector cannot afford an incoming rate of 40 MHz . In the upgrade, infact, all the read-out will be substituted and the *L0* trigger will be replaced by a software one.
- *High Level Trigger (HLT) and Offline reconstruction*: the HLT consists in an *Online* software trigger where the full reconstruction of tracks is performed. It's at this level that the tracking algorithms are run. After the HLT, data are stored and an *Offline* reconstruction is also performed before providing usable object for data analysis.¹ Finally data are *stripped*, meaning that additional cuts are applied before their conversion in usable objects for data analysis.

¹During the Run-I, the seeding algorithm (called *PatSeeding*) in the HLT was run making use of the left-over hits coming from the *Forward* algorithm. During Run-I the *Seeding* was used in the online reconstruction in tandem with the *Forward* as described before while in the offline reconstruction it was run as a *Standalone* algorithm. For the Run-II online and offline reconstruction gives more or less the same results, but, anyway, the seeding algorithm remains one of the most important one.

- *LHCb* luminosity is kept constant and it's reduced with respect to other *LHC* experiments of 2 orders of magnitudes. This reduction in luminosity is achieved thanks to the *Luminosity Levelling* mechanism². This reduction of luminosity is mandatory since the main studies on *b* and *c* hadrons require an extraordinary precise reconstruction of the production vertices of the produced and decaying particles, so, the Vertex Locator (*VELO*) can be placed at very small distance from the interaction point limiting problems coming from radiation damages.³

In table 1.1 (where ν stands for the average number of visible interaction per bunch crossing) a comparison of the current *LHCb* and the upgrade one is shown.

	Current <i>LHCb</i>	Upgrade <i>LHCb</i>
Trigger	Hardware(<i>L0</i>) + Software(<i>HLT</i>)	Only Software
Read-out rate	<i>L0</i> : 40 MHz to 1MHz for readout	40 MHz Full software trigger for every 25 ns bunch crossing
Luminosity	$4 \times 10^{32} \text{ cm}^{-2} \text{ s}^{-1}$	$2 \times 10^{33} \text{ cm}^{-2} \text{ s}^{-1}$
ν	2	7.6

Table 1.1: Main differences between actual *LHCb* and the Upgrade

The reason why the *L0* trigger will be removed in the upgrade is mainly because some of the analysis looking for deviations from Standard Model are limited by statistics and a fixed 1 MHz readout at the upgrade running condition will be too limiting. To be precise, channels containing hadrons in the final state are the one who suffers the most the *L0* hadron trigger. In order to reach the physics goals the *LHCb* detector will be upgraded and the installation of the new detectors and the new read-out is expected to happen during the long shutdown 2 in 2018/2019. Each subdetectors will be replaced as shown in Fig. 1.1.

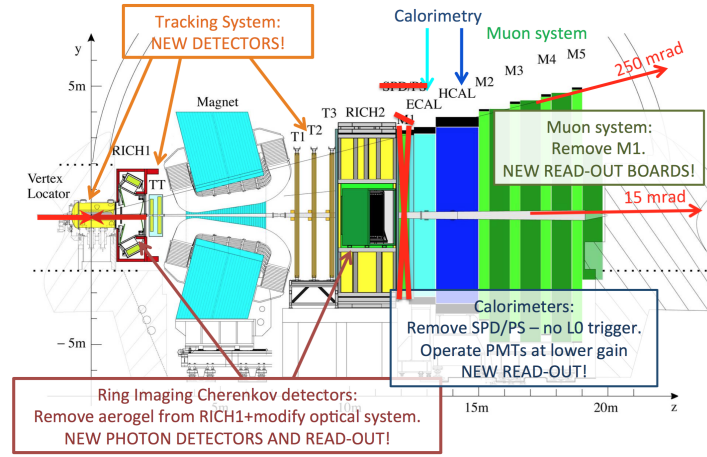


Figure 1.1: *LHCb* detector modifications for the upgrade. The Vertex Locator (*VELO*), the Tracker Turicensis(*TT*) and the 3 T-Stations are the main responsible of the tracking at *LHCb*. The Particle Identification is ensured by the two ring cherenkove detectors (*RICH1* and *RICH2*). The particles energy measurement is provided by the hadronic and the electromagnetic calorimeters (*HCAL* and *ECAL* respectively). The properties of the muons are then mainly determined by the Muon System.

The *VELO* will be replaced by a lightweight hybrid pixel detector capable of 40 MHz readout at the upgrade luminosity which is 5 times greater than the actual one. The trackers placed downstream and upstream with respect to the magnet will be also completely replaced to cope for the higher luminosity, higher occupancy and the 40 MHz read-out.

Another reason why it's necessary to replace them is related to the fact that for the upgrade phase of *LHCb* an integrated luminosity greater than 50 fb^{-1} is expected to be collected and the detector itself is required to be resistant to the corresponding radiation damages.

The adopted solution for the downstream magnet upgrade is the *Scintillating Fibre Tracker (SciFi)*. The active and light-transport (also wavelength shifter) material for the detector are the fibres themselves and the read-out is provided by arrays of silicon photomultipliers. The pitch of a single channel is designed to be equal to $250 \mu\text{m}$ and each module of the detector consist of 5 (6 in central region) closed packed fibres ($\Phi \sim 250 \mu\text{m}$) layer.

The *SciFi* is placed in the downstream region with respect to the magnet (*B* field lines direction are along the *y* direction) and it consists of 3 stations, *T1*, *T2*, *T3*. *T1* (placed at $z \sim 8\text{m}$) is the one closer to the magnet while *T3* (placed at $z \sim 10\text{m}$) is the one closer to the calorimeter. Each station is composed of four layers of scintillating fibres detectors oriented in the so-called *x-u-v-x* configuration.⁴

This configuration (*x-u-v-x*) allows the reconstruction of tracks using their projection in the bending *x-z* plane and *y* information obtained through the combined measurement of the *u-v* layers.

Each layer is divided in two halves (roughly $y > 0$ and $y < 0$) equipped at $y=0$ by a mirror to improve the light yield in the higher occupancy area (the region close to the beam pipe).

²The *Luminosity Levelling* avoid head-on collisions separating beams perpendicularly to the collision plane.

³The decrease from the maximal designed luminosity of *LHC* of $10^{34} \text{ cm}^{-2} \text{ s}^{-1}$ to the *LHCb* one $10^{32} \text{ cm}^{-2} \text{ s}^{-1}$ permit to reduce the average number of inelastic collisions from 27 to 0.53 and it allows to reconstruct with extraordinary precision the primary vertices.

⁴The *x* - layer contains fibres oriented perpendicularly to the *x-z* plane while the *u(v)* layers are exactly the same as the *x*-layers but rotated by a "stereo" angle of ± 5 degree in the *x-y* plane in order to reconstruct also the *y*-information of the tracks.

A view of how a single station look like is given in 1.2 and it will consists of around 10.000 Km of fibres and 560.000 read-out channels distributed over the 12 layers (6 x , 3 u , 3 v).

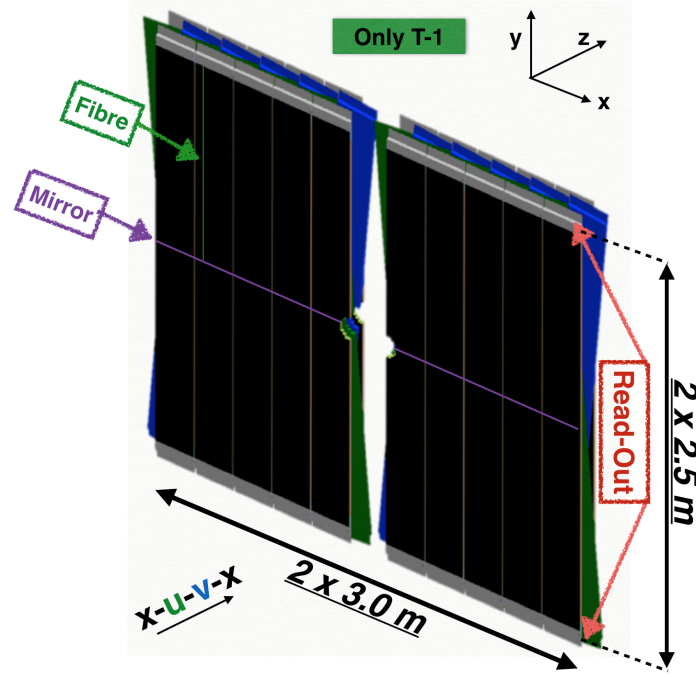


Figure 1.2: Sketch of a single station of the SciFi tracker. Each station is made of 4 different layers in x - u - v - x configuration, the central region is mirrored and the read-out is done at the edges of the layers far from the beam pipe.

The requirements for the SciFi to satisfy the physics program of *LHCb* can be listed in few concise points:

- The hit efficiency has to be $\sim 99\%$.
- The noise cluster rate should be less than 10%, reason why the *SiPM* read-out has to be cooled
- The position resolution in the bending plane has to be $\sim 100\mu\text{m}$ and the material budget has to be as reduced as possible $\frac{X}{X_0} < 1\%$ per detector layer.
- The read-out has to be performed at 40 MHz.
- The tracker has to be efficient for at least an integrated luminosity of 50 fb^{-1} .
- The SciFi tracker has to replace the actual one, so additional geometrical constraints must be satisfied.

1.2 PATTERN RECOGNITION AT LHCb

The track reconstruction at *LHCb* is performed in different steps.

The first one is a local search of tracks, and it's done looking to hits in each subdetectors. Since the magnetic field is different depending on the region where we are looking at, some assumptions on the magnetic field shape has to be done. These assumptions are directly translated to the track model to use in order to find the tracks.

For example, the track model used in the *Velo* algorithm consists in a straight line since the magnetic field is almost zero in the *Velo* region, while if we assume the B field to be constant in a given region, the track model is a parabola.

So, the main goal of this first step is to have reasonable objects (collection of hits) which can be identified as potential good tracks, given the properties of the detector and the magnetic field. These candidates are stored in different output containers related to the different algorithms.

The second step consists in a global fit performed once the list of potential good tracks are found. This step relies on the *Kalman Filter* and a *Ghost and Clone killer* procedure.

We will then refer to the first step as *pattern recognition* and the second one as the *final fit*.

The pattern recognition at *LHCb* is done depending on the path the track goes through, so it's based on the detector's hit content as shown in Fig. 1.3.

In the tracking system of *LHCb* each track type is reconstructed by a dedicated algorithm as summarised in table 1.2.

All the tracks produced by the algorithms provided in table 1.2 are processed afterwards by the *Kalman Filter* which fit the tracks assigning a χ^2 value to the tracks which is different from the χ^2 provided by the algorithms of the *pattern recognition* step.

Each algorithm has in fact an internal track model parametrisation and the global effect comparing different algorithms is to have different χ^2 value for the same track.

⁵ z - is the beam axis direction and the y axis is the B field line direction.

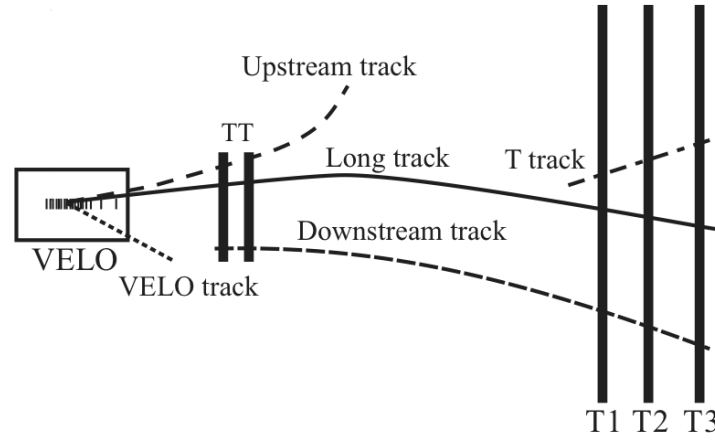


Figure 1.3: Track type at LHCb. Velo tracks are basically straight lines since the magnetic field is almost 0 in that region. Tracks are mainly bended in the x - z plane between the Tracker Turicensis (Upstream Tracker for the upgrade) and the T-Stations which is composed by the Inner Tracker (IT) and the Outer Tracker (OT) (Run-I and Run-II), while for the upgrade the stations will be replaced by the Scintillating Fibre tracker (SciFi).

Track type	Used detector	Algorithm(s)	Input tracks	Output tracks
Velo Tracks or Velo-Segment	Velo	Velo algorithm	/	Velo
Seed Tracks or T-Tracks	T-Stations (SciFi in upgrade)	Seeding algorithm	Allow the possible usage of the leftover hits of forward. If Not: Standalone Algo	Seed
Long Tracks (1)	Velo + TT + T-Stations (TT \rightarrow UT T-Stations \rightarrow SciFi in upgrade)	1) Forward tracking: Search in T-Stations knowing Velo-Segment (adding also TT) 2) Matching algorithm: Merge T-Tracks with Velo-Segment 3) BestSelector= Forward+Matching	Velo Velo and Seed	Long
Downstream Tracks	T-Stations and TT (SciFi and UT)	Downstream algorithm: Use T-Tracks and add TT (UT upgrade) hits	Seed	Downstream
Upstream Track	Velo and TT	Upstream algorithm: Use Velo segment and add TT (UT upgrade) hits	Velo Container	Upstream

Table 1.2: Pattern recognition at LHCb

Differently from pattern recognition, it's the *Kalman Filter* the algorithm where the fit procedure takes into account the full $B(x,y,z)$ field map and the material budget computing the corrections due to multiscattering.

From a more technical point of view, in the *Kalman Filter* and in the *LHCb* framework each track is defined by a vector of track state $\left(x, y, t_x, t_y, \frac{q}{p}\right)^T_z$ where $t_x = \frac{dx}{dz}$ is the slope of the track in the x - z plane at a given z , $t_y = \frac{dy}{dz}$ is the slope of the track in the y - z plane at a given z . In the *Kalman Filter* the track state is propagated by a 5x5 matrix through the detector considering the interactions in the material and the magnetic field map⁶.

The main goal of the pattern recognition algorithm in Table 1.2 is to provide a preliminary set of tracks made by compatible hits in a given sub-detector. Only at the end of the algorithms the found tracks (or, better, set of hits) are converted into a vector of track states, which can be handled by the *Kalman Filter* and the *Ghost and Clone Killer*.

1.3 HYBRID SEEDING ALGORITHM

In order to figure out the limitations, exploit the future performances and eventually improve the baseline detector layout of the *SciFi* tracker, a huge effort must be done to reproduce what the real data taking conditions together with the real output of the detector would be.

This task is obtained through different steps in the *LHCb* simulation software. Without going into details we can make a short summary of how the *LHCb* software is working in order to provide, for a given algorithm the final efficiencies. In this document reconstruction efficiencies are estimated for a simulated sample of $B_s \rightarrow \phi(K^+K^-)\phi(K^+K^-)$ event.

- *Gauss*: this application is responsible of the physics simulation, starting from the pp collisions (the package doing that is called *Pythia8*). For the upgrade the 25 ns bunch crossing, $\sqrt{s} = 14$ TeV centre-of mass energy collision and the $v=7.6$ are passed

⁶The formalism is quite similar to accelerator physics for beam transport.

as argument. After the collision simulation the subsequent $B_s^0 \rightarrow \phi(K^+K^-)\phi(K^+K^-)$ decay is simulated (this is done in the *EvtGen* package). Inside *Gauss* also the interaction in material of the produced final states in the detector is simulated by the *Geant* package. At this level of the simulation the so-called *MCHits* are produced, corresponding to the energy deposition in the active material of the detector. A true particle is then given by a certain set of *MCHits*.

- *Boole*: this application is responsible for simulation the light attenuation, the *SiPM* response read-out, the *clusterisation*, the final read-out (data - encoding). The output of this step are the *Clusters* containing binary information about the corresponding position in the tracker and additional information of the cluster such as the *charge* and the *cluster size*.
- *Brunel*: once the digitization is done, the resulting objects that the pattern recognition algorithms can handle are the so called *PrHit* (in the *SciFi* context) and making use of them one can finally reconstruct tracks. The *PrHit* are obtained converting the binary information of the *Clusters* into a geometrical information usable for pattern recognition. The track reconstruction is done inside the *Brunel* application. It's clear that, if something goes wrong in the digitization or in the detector geometrical information description, the pattern recognition algorithm will fail in the reconstruction, resulting in loss of tracking efficiencies.
- *Brunel checkers*: in order to provide the tracing reconstruction efficiencies, it is important to propagate the information of what we suppose to reconstruct if the pattern recognition algorithm would be 100% efficient. To do that, we store the *Linkers* inside *Boole* in order to figure out the list of *MCHit* associated to the same true particle ending up into a *Cluster*, i.e., into a *PrHit*. Thanks to these *Linkers* one can define the *reconstructible*⁷ tracks and comparing them to the output of the pattern recognition algorithm (*reconstructed* tracks) we are able to provide the pattern recognition efficiencies.

The most important figures of merit used to evaluate the performances of a pattern recognition algorithm are the following:

- *Reconstruction efficiency*: The track finding efficiency is defined as the fraction of MC particles in the acceptance that are successfully reconstructed, i.e., the percentage of *reconstructed* tracks which are MC-matched (sharing the 70 % of hit) among the set of *MCParticles* ending in the *LHCb* acceptance.

$$\epsilon = \frac{N_{MC-matched}}{N_{MC-acceptance}}.$$

The acceptance is defined as at least one *x* and one *u* or *v* layer hit per station.

- *Ghost rate*: It is defined as the fraction of ghost tracks among the set of *reconstructed*, i.e., as the fraction of *reconstructed* tracks not matched to a *MCParticle*.

$$ghost_{rate} = \frac{N_{ghost}}{N_{reconstructed}}.$$

Ghosts are generated from pseudo-random combination of hits. This parameter is important because we don't want to reconstruct fake tracks or use them in analysis, and, in addition, we don't want to feed the *Kalman Filter* with too many fake tracks due to timing constraints.

- *Timing*: It is defined as the time we spend to find the tracks in the algorithm. This is particularly important for the upgrade since the pattern recognition algorithms will run online at an incoming rate of 40 MHz.

The work done from October 2014 to now is based in this framework.

At the beginning i was involved in the debugging of the simulation code (*Boole* and *Brunel*), in the detector description, the clusterisation and the encoding and decoding of the clusters to figure out the presence of some inconsistencies or wrong assumptions.

Some problems and inefficiencies in the software were not well understood passing from the default detector description (the one used for the Technical Design Report [4]) to the new one where bigger gaps between channels were simulated, together with a new shape of detector layers, and a more realistic model of the clusterisation.

In that context my effort was crucial (I took part to the “*DILBERT*” task force for the software fixing and bug correction) to recover part of the loss in efficiency. A stable version of the detector simulation was released and starting from that, the development of a new pattern recognition algorithm becomes possible.

The discrepancies in efficiencies with the *TDR* values were understood: increased dead region due to the gaps in between two different readout channels leads to a loss in efficiency or around 2% which is what is shown in 1.3 comparing the first and the third column.

In the meanwhile i participated the *test beam* data taking and data analysis aiming to measure the attenuation length of the fibres doing light yield measurements scanning along the active material at different distances from the read-out and also evaluating the dependency of the cluster size against track incident angles. I also analyse some of the data from the test beam to study the cluster size properties as a function of the incident angle of tracks in the detector in order to tune the simulation to be the most reliable and realistic possible. [6] [7].

The results of how the efficiencies for the seeding algorithm evolved since i started will be shown at the end of this section to highlight my contribution to the upgrade *SciFi simulation and reconstruction* working group. I presented regularly my work in the internal *SciFi simulation and reconstruction* working group and i presented once the results of the group in the parallel session of the *LHCb week*. The list of talks and presentations done will be listed in the talks and presentations section.

⁷For the *SciFi* a reconstructible track is defined if it leaves at least 1 x-layer hit in each of the three stations together with at least one hit in the u or v layer for each of the three stations.

1.4 IMPROVEMENTS TO THE ALGORITHM

Several studies has been performed for the previous algorithm (referred to *Old* here) in order to understand and improve it. Once we figured out the limitations of it we decided to develop a new one from scratch. The development of the new one started from very basics things related to track properties, detector occupancy and requirements on tracks. First of all we need to separate different aspects of the algorithm:

- The way we collect the hits to generate tracks.
- The way we fit the tracks.
- The tolerances we allow in both the fitting and the hit search.
- The requirements we put on tracks for their storage and clone/ghost killing.

In order to do that, several tools have been developed: one of them, for instance, aims to extract the true *Monte-Carlo* information of tracks before the clusterisation step in order to evaluate the track properties and their behavior in the *SciFi* stations.⁸

The strategy adopted once the track property was extracted was then following: instead of using a look-up table for the B field information one can directly use the B -field effect on tracks parametrising their motion by some fixed constants reflecting the magnetic field behavior.⁹

The main improvement from this study was the introduction of a new track model and the evaluation of some fixed parameter describing the motion of the tracks and their properties (*pointing* to the origin vertex). The adopted track model is the following:

$$x(z) = a_x + b_x \cdot (z - z_{ref}) + c_x \cdot (z - z_{ref})^2 \cdot (1 + dRatio \cdot (z - z_{ref}))$$

$$y(z) = a_y + b_y \cdot (z - z_{ref})$$

where $dRatio$ is a fixed term resulting from a linear decrease along z of the magnetic field along y direction (the farther we are from the magnet, the smaller is the magnetic field). The terms in the model a_x and a_y are respectively $x(z_{ref})$ and $y(z_{ref})$ resulting from the solution of the equation of motion. In the same way one can find out that $b_x \propto \frac{q \cdot p_x}{p_z}$ ($b_y \propto p_y$) and $c_x \propto \frac{q}{p_z}$.

The track model in the non-bending plane (y - z) is a straight line because the magnetic field along z and x is almost zero and it should not affect at all the track motion. Mathematically, the resulting track model is the direct consequence of the assumption for which the magnetic field is given by

$$\vec{B} = (0, B0(x, y) + B1(x, y) \cdot z, 0).$$

plus the addition of the fixed term

$$dRatio = \frac{B1(x, y)}{B0(x, y)} = const.$$

which is a very good assumption for tracks going through the central region of the detector ($|x| < 1000\text{mm}$ and $|y| < 1000\text{mm}$) while it becomes false if the tracks goes through the fringe field region corresponding to the external parts of the detector ($|x| > 1000\text{mm}$ and $|y| > 1000\text{mm}$) where the occupancy is much smaller and looser requirements can be applied.

Another improvement introduced in the algorithm concerns the possibility to estimate the origin vertex position ($x_{track}(z=0)$) accounting for the average bending the particles experience when they travel from the *Velo* to the z_{ref} . This is encoded in the *backward projection* parameter estimated as $X_0 = a_x - b_x z_{ref} + c_x \cdot C$ where C is fixed from *MC* studies and it is related to

$$C = \int_0^{z_{ref}} dz' \int_0^{z'} B_y(z) dz$$

and the other parameters are the one one would find from the fit. Since the largest part of tracks we detect comes from the origin vertex, the *backward projection* becomes extremely usefull in the ghost rejection.

The main limitations, or problems, of the previous algorithm can be summarized in few points:

- It was trying to find everything at once, meaning that it was not disentangling the cases where tracks are easy to find to the cases where the tracks are harder to find. Harder to find stands for find it paying an high prize in terms of ghost rate. This is related to two different aspects: the intrinsic properties of the track, such as its momentum as well as the detector occupancy.
- The tracks behavior in the *SciFi* tracker was roughly parametrised, no $dRatio$ correction.
- The different detector area were treated in the same way. For example it was not taking into account that where we expect to have a lower occupancy we can loosen the cuts for the track selection.

The strategy adopted for the track search is to **split the algorithm in nested sub blocks** following the philosophy of the *projective tracking* and *progressive cleaning* of the tracking environment. Since the detector is divided into two halves ($y > 0\text{mm}$ and $y < 0\text{mm}$) a natural choice is to split the algorithm in a first step where tracks are searched for using only the hits in the upper modules of the stations and a second iteration is done using hits from the lower half. From the *MC* study we find out that the amount of tracks going from the upper to the lower half is a negligible fraction of the full set of tracks $\sim O(0.1\%)$.

⁸Thanks to that a tracking algorithm running over true hit position was developped to figure out which is the best track model to use in order to fit the tracks going through the *SciFi* and also to have an estimation of "how much" one can squeeze some search windows without starting to loose too much in efficiencies.

⁹The B field in the *Sci-Fi* tracker region is a fringe field which is not easily parametrisable, but still, some caracteristic behavior can be extracted.

Inside the upper(or lower) half search we run the second main block of the algorithm three times (we will call them *cases*). The idea of splitting the algorithm in three *cases* is related to the fact we want to firstly find the easier tracks (high momentum one), mark the hits associated to them and look for more complicated tracks (lower momentum, highly curved tracks) in a cleaner environment. This is obtained through different configurations for search windows and tolerances inside each *case*.

Strictly speaking, the first case aims to find high momentum tracks ($p > 5$ GeV) while the second and the third *case* aims to find tracks with $p < 5$ GeV which are harder to find (higher search windows and looser χ^2 cuts) and also complete the search for high momentum tracks which are not found by the first *case*.

Each one of the *case* is then dependent on the previous one since at the end of each of them (only the first and the second) we mark the hits on the found tracks using some specific criteria making them unavailable for the following *case*.

The net result is a progressive cleaning of the tracking environment moving from one case to the following one. For example in the second *case* the hits found by the first one are not available for track reconstruction.

Each of the case is made by some different step:

- ***x-hit search***: Hits are collected using only the x layers in the 3 stations, so the maximal number of hits on track is 6 and the minimal one can be set to 4 or 5 depending on the case. The lower is the minimal number of hit required here the higher is the ghost rate since, for instance, tracks with only 4 x -layer hits are much less constrained than tracks with 6 x -layer hits.
 1. 2-Hit combinations are obtained looking at pairs of hits in the x -layers in $T1$ and $T3$. Given a hit in the first station ($T1$) the infinite momentum prediction is used to open a search window in $T3$ ($x_{T3} \sim \frac{x_{T1}}{z_{T1}} \cdot z_{T3}$ under the p^∞ assumption). All possible 2-hit combination are then collected. Tighter search window is applied for the first *case* and bigger ones are used for the second and third one in order to find lower momentum tracks.
 2. Any possible (in within a given tolerance) third hit from $T2$ is added to each single pair taking the linear prediction from $x_{T2} = \frac{x_{T3} - x_{T1}}{z_{T3} - z_{T1}} \cdot z_{T2}$. At this step, the smaller is the momentum of the track we are searching for and the bigger the deviation from the linear predicted position we should look for. This search window is correlated to the p_x and to the sagitta of the track itself in the bending plane.
 3. Given the three hit combination (one per station), the parameters of a parabola can be computed solving for a_x, b_x, c_x form the linear system given by $x_i(z_{T-i}) = a_x + b_x \cdot dz_{T-i} + c_x dz_{T-i}^2$ where $dz_{T-i} = z_{T-i} - z_{ref}$ and z_{ref} is picked to be $8530mm$ ($\sim z_{T2}$) for numerical stability of track parameters (a_x, b_x, c_x).¹⁰
 4. Once we have the a_x, b_x and c_x we can compute the predicted x position at any z and collect the found hits around the expected position inside a given tolerance. At this step the hit at the smallest distance from the prediction is picked and added to the track.
 5. At this stage, a list of hits is collected which should correspond to the x - z projection of the true track in x -layers.
 6. A track object is created using the hits found in the *SciFi* and a fit is performed. The fit uses as track model for the x - z projection the following parametrisation $x(z) = a_x + b_x dz + c_x dz^2 (1 + dRatio \cdot dz)$.
 - a) The *Backward projection* X_0 is computed, being the estimation of the $x(z = 0mm)$ accounting for the integrated magnetic field from $z = 0$ to $z = z_{ref}$ under the assumption that the particle is generated at $(x = 0, z = 0)$. The formula used is then $X_0 = a_x^{fit} + b_x^{fit} + c_x^{fit} \cdot C^{Const}$ where C^{Const} is a fixed parameter found from simulation accounting for the kick that the tracks receive in the region before the *SciFi*.
 - b) Combined cuts are applied in the plane given by the χ^2 versus X_0 to return the fit status. At this step also the occupancy is taken into account. For tracks going far from the beampipe ($|X_{T1}| > 500mm$) looser cuts are applied since the chance to find compatible hits in the **stereo hit search** step is much lower than in the higher occupancy detector area ($|X_{T1}| < 500mm$).
 - c) If the x - z *projection* of the track satisfy the requirements they are stored as good tracks, if not, they are *refitted* after the removal of the worst hit (defined as the hit giving the higher contribution to the χ^2). So, for example, if we find a x - z *projection* track with 6 hit and at the first fit the fit is not successful because of the requirements we put on the χ^2 and the X_0 , we remove one hit and we refit it again. This process is done recursively as soon as we don't reach the limit given by the minimal number of hits we require. At this step of the fitting and minimal hit requirements, we make some differentiation between the first *case* and the following ones. For example, in the first and the second *case* we keep only tracks containing 4 hits on x layers at the second and the third iteration of the *fit* while for the third *case* we also keep 4 hits on track at the first iteration.
 7. The tracks are stored (at this stage we can only have tracks containing 4,5 or 6 hits) and a *clone removal step* is performed based on a minimal number of shared hits, which is set to 2 by default. If two tracks shares 2 hits or more, we keep the one with the higher number of hits, if they have the same amount of hits, we keep the one with the better $\frac{\chi^2}{ndof}$.

- **Stereo hit search**

1. For each of the x - z candidates found in the x - z *search* step, a list of compatible hits in the u - v layers is collected once the x predicted position x_{pred} is computed using the usual track model $x(z) = a_x + b_x \cdot dz + c_x \cdot dz^2 (1 + dRatio \cdot dz)$. Since the $u(v)$ layers have the fibres bended in the x - y plane of $\alpha = +5^\circ$ ($\alpha = -5^\circ$) what can be actually handled in the algorithm is the $\frac{u - x_{pred}}{\sin(\alpha)}$ which is related to the y position we allow.
2. Once a vector of compatible hits in within the y tolerance we set is created, the collected hits are sorted by β , where the $\beta_{Hit} = \frac{u - x_{pred}}{\sin(\alpha) z_{Hit}} \sim \frac{y}{z}$.

¹⁰In reality we solve for (a_x, b_x, c_x) using $x(z) = a_x + b_x dz + c_x dz^2 (1 + dRatio \cdot dz)$ where the $dRatio$ is fixed by MC studies

3. Since the magnetic field is almost zero in the x and z direction the track motion is basically a straight line in the non-bending plane y - z . So, if a group of hits have the same β this is a hint that we are actually finding a good combination of stereo hits to add to our x -*candidate*. Infact, what we pass to the fitting method is the track created by the x - z candidate plus all the hits satisfying $\beta_{Hit_i} - \beta_{Hit_j} < \text{ToLerance}$. This is the way the *hough transformation* “like” is implemented¹¹.
4. For each of the track candidates we generate adding the stereo hits, we make a fit and , as in the x - z *projection* search, a fit is performed, but at this stage the track model is extended also to the y - z plane. The adopted model becomes then

$$\begin{cases} x(z) = a_x + b_x dz + c_x dz^2 \cdot (1 + dRatio \cdot dz) \\ y(z) = a_y + b_y z \end{cases}$$

5. In the fit method the status of the fit (failed or successful) is based on different properties: the maximal contribution of the hit to the χ^2 , the χ^2 of the track, the number of hits on the track, the value of the backward projection X_0 , the value of the y backward projection (i.e. $\text{track.y}(z=0 \text{ mm})$ and the region of the detector interested ($x(zT1), x(zT3), y(zT1), y(zT3)$). The last bit is taken into account because knowing where the track is going through in the detector we can apply stronger requirements for tracks going through the higher occupancy area, reducing the ghost rate.
 - a) If the track satisfies the requirements, it is stored in memory as a good candidate, if not, we remove the worst hit and we redo the fit.
6. Since the starting point is an x -*Candidate* and there is the possibility to find more than one stereo segment associated to that, the best one is selected, based on the number of hits on track (favouring the one with more hits) and keeping the one with the best $\frac{\chi^2}{ndof}$ if the comparison is done between the same amount of hits on the track.

- Once we have the track candidates produced by the *Case* tracks undergoes a clone removal step which has the same logic as the one in x - z search.
- As discussed, the algorithm is sub-divided in 3 *Case*, and the passage between the first one and the next is done performing a “*Flagging*” of the hits found on the tracks associated to the case. The flagging step has a crucial role in the *progressively cleaning* of the tracking environment because the algorithm is re-run without considering the hits found in the previous case.¹²

Depending on the *case* different selection windows and selection cuts are applied in order to firstly find the tracks with higher momentum ($p > 5 \text{ GeV}$) which are the easier to find and later we search for tracks with lower momentum. The correlation between easier and harder to find is related to the search windows to open in the x - z *search* especially in the very first step of the 2-Hit search. This is due to the kick the tracks get from the B field in the *SciFi* tracker region which is $\propto \frac{B}{p}$. In addition the *pointing* to the origin vertex given by the X_0 and $\text{track.y}(0)$ is much more accurate for higher momentum tracks.

The infinite momentum assumption relies on the fact that very high momentum tracks motion is almost a straight line in the x - z bending plane, resulting in a linear pointing to the origin vertex ($(x,y,z)=(0,0,0)$). Of course, not all the tracks originate from the primary vertex, anyway, the assumption is still good enough to find high momentum K_S^0 daughters, since they are produced almost collinearly with the K_S^0 .

There is a work in progress to document the new algorithm in order to provide a detailed description of all the technical implementation of it, to check the robustness of it and there are also some additional ideas to apport in order to get better efficiencies.

The preliminary results obtained by running on 1000 events of $B_s \rightarrow \phi\phi$ are given in table 1.3 comparing them to the evolution of the efficiencies for the *upgrade seeding algorithm* since i started to work on this subject.

As it can be observed a huge improvement has been apported to the *seeding* algorithm since the *TDR* time.

We should underline that at the *TDR* time the gaps between the read-out channels were smaller (hit efficiency difference $\sim 1\%$) than the one implemented later on ($2^{nd}, 3^{rd}, 4^{th}$ column) resulting into an expected $\sim 2\%$ difference in tracking efficiencies. As it can be observed, moving from one detector description to the more realistic one (1^{st} versus 2^{nd} column) the drop in efficiency was too high to be only related to the additional dead regions introduced in the simulation. The gap has been reduced thanks to the *debugging* work described at the beginning (2^{nd} versus 3^{rd} column) and the new algorithm has been started to be developed (last column).

As it can be observed, a postive improvement for all the track category has been obtained and, more remarkably, a much lower ghost rate has been obtained. Further improvements are expected to be put in place such as the introduction of a position dependent ,i.e. $dRatio(x, y)$ correction and also a better track comparison procedure in order to kill the ghosts and the clones without losing in efficiency.

1.5 ANALYSIS WORK : $B^0 \rightarrow D^0 \bar{D}^0 K^{*0}$ ANALYSIS

The subject of my thesis is the study of double charm B decays at LHCb. The planning of the analysis is the following:

- Provide the first observation of $B^0 \rightarrow D^0 \bar{D}^0 K^{*0}$ using as reference channel $B^+ \rightarrow D^0 \bar{D}^0 K^+$ measuring its $\mathcal{B}\mathcal{R}$.. The main reason why we need a reference channel in this measurement is because lot of systematics effects on the measurement can be neglected in that way.

¹¹The technical implementation is the followign: we pick the first hit in the β sorted array and we go at the sixth element after it in the array. If it satisfy the tolerance condition we extend the picked hits from 6 untill the $\beta_{Hit_i} - \beta_{Hit_j} < \text{Tolerance}$ is not satisfied anymore. If the search fails we move in steps of 6 inside the array and we repeat the search

¹²Each case is carachterized by the selection of the 2-hit combination: where for case 1 we have small search windows since we are trying to reconstruct high momentum tracks which are the easiest one to build.

Track Type	TDR	Old Seeding (when i started)	Old Seeding (after task force)	Hybrid Seeding (Δ)
hasT	66.1 %	53.2 %	64.1 %	76.7 % (+12.1 %)
long	82.2 %	73.0 %	79.9 %	88.3 % (+8.4 %)
long > 5 GeV	88.7 %	82.6 %	87.2 %	92.8 % (+5.6 %)
long fromB	87.6 %	79.8 %	85.1 %	90.7 % (+5.6 %)
long fromB > 5 GeV	90.5 %	85.3 %	89.1 %	92.9 % (+3.8 %)
UT+T Strange	79.2 %	68.5 %	76.7 %	86.9 % (+10.2 %)
UT+T Strange > 5GeV	88.8 %	83.0 %	86.7 %	92.8 % (+6.1 %)
noVelo+UT+T strange	80.4 %	70.1 %	78.2 %	87.2 % (+9.0 %)
noVelo+UT+T strange > 5GeV	88.6 %	83.5 %	86.6 %	92.8 % (+6.2 %)
UT+T SfromDB	79.4 %	70.2 %	78.9 %	88.3 % (+9.4 %)
UT+T SfromDB > 5GeV	90.9 %	84.1 %	88.7 %	94.1 % (+5.4 %)
noVelo+UT+TfromDB	78.9 %	68.4 %	81.1 %	85.8 % (+4.7 %)
noVelo+UT+T SfromDB > 5GeV	88.6 %	84.1 %	89.1 %	94.5 % (+5.4 %)
Ghost Rate	18.0 %	28.6 %	21.2 %	10.1 % (-11.1 %)
Hit Efficiency(hasT)	96.43 %	94.97 %	95.1 %	92.4 % (-2.7 %)

Table 1.3: *Efficiencies numbers for the seeding algorithm since i started working on it. TDR numbers are obtained with a less realistic detector description and with a simplified clusterisation. The second column are the efficiencies values at October 2014 after the implementation of a new detector description and modifications in the digitisation algorithm. The third column are the efficiencies values after the correction of bugs we find in the code related to the detector description and the digitisation. The last column are the efficiencies for the seeding algorithm developed. Efficiencies here are given for 1000 events of simulated $B_s^0 \rightarrow \phi(K^+ K^-)\phi(K^+ K^-)$ accounting for tracks in $\eta \in [2, 5]$ and without taking into account the electrons.*

- Amplitude analysis of $B^0 \rightarrow D^0 \bar{D}^0 K^{*0}$ using *Dalitz analysis* techniques. The goal of this study is to figure out if some exotic resonance (*XYZ*) states are present in the spectrum of the $D^0 \bar{D}^0$ invariant mass.

Unfortunately i was not able to work on that since October 2014, but some preliminary study has been carried out and a clear idea of how to proceed has been put in place as it will be described in the timetable for future plans section. Anyway, a preliminary work as been done, mainly regarding the reference channel, i.e. $B^+ \rightarrow D^0 \bar{D}^0 K^+ + c.c.$, where *C.C.* stands for charge conjugate decay channel. As already said the first goal is the measurement of the branching ration for $B^0 \rightarrow D^0 \bar{D}^0 K^{*0} + C.C.$ (never measured and observed so far) using the $B^+ \rightarrow D^0 \bar{D}^0 K^+ + C.C.$ as reference channel. The D mesons are reconstructed through $D^0 \rightarrow K^- \pi^+ + c.c.$

The B mesons double charm decays have been introduced to explain the discrepancy between the semileptonic branching ratio of B decays and the observed number of charmed mesons in B decays. Nowadays, there are some of the decay modes which have not been observed and $B^0 \rightarrow D^0 \bar{D}^0 K^{*0}$ is one of them. More interest about this topology of decay concern the search of exotic structures above the open charm thresholds ($> 2M_D$). In this invariant mass region observed states and charmonium ($c\bar{c}$ bound states) predicted one are in disagreement and channels as the one considered for my thesis can lead to interesting results in this domain.

1.5.1 $B \rightarrow D^{(*)} D^{(*)} K^{(*)}$ DECAYS : TOPOLOGY AND POSSIBLE PHYSICS STUDIES

At the quark level, the $B^+ \rightarrow D^0 \bar{D}^0 K^+ + c.c.$ $B^0 \rightarrow D^0 \bar{D}^0 K^{*0} + c.c.$ are generally described by the *CKM* favoured weak transition $\bar{b} \rightarrow \bar{c} W^+ \rightarrow \bar{c} c \bar{s}$ with additional $u\bar{u}$ (or $d\bar{d}$) quarks coming from the *QCD* vacuum.¹³ The relevant diagrams for such decay modes are shown in Fig 1.4.

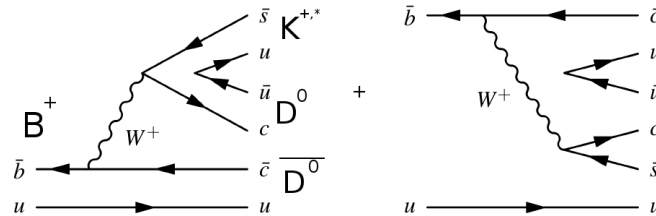


Figure 1.4: *Leading order feynman diagrams for $B^+ \rightarrow D^0 \bar{D}^0 K^+$. On the left the colour-favoured mode ($u\bar{u}$ from QCD vacuum can have 3 different colour assignment), on the right the colour suppressed mode (once the spectator quark colour is fixed, all the others are fixed). For $B^+ \rightarrow D^0 \bar{D}^0 K^+$ both the modes can occur while for the $B^0 \rightarrow D^0 \bar{D}^0 K^{*0}$ only the suppressed mode can occurs.*

Hadrons are colourless objects so the decay modes containing $D^{(*)}$ as the ones of interest are produced in majority through

¹³These decay modes have been introduced due to the so called *Charm counting puzzle*, i.e., theoretical discrepancy between the semileptonic branching ratio of B decays with the number of charmed hadrons produced in B decays.

Internal (colour suppressed) and/or external modes (colour favoured). The reference channel occur through both of them while the $B^0 \rightarrow D^0 \bar{D}^0 K^{*0}$ only internally.

The major study, which can be done through these decay modes, is the spectroscopy of $c\bar{s}$ and $c\bar{c}$ states. Resonances coming from $D_s^* \rightarrow D^{(*)} K^{(*)}$ and $X \rightarrow D^{(*)} D^{(*)}$ can be studied in 3-body decays through *Dalitz Amplitude Analysis technique*. The physics case is more interesting for the second category.¹⁴ The weak decay of interest is isospin conserving, so through isospin decomposition of amplitudes one can also test the factorization theorem for three body decays and predict the branching ratio of other similar channels just measuring one of them.

1.5.2 ANALYSIS PERFORMED

The goal of the analysis is to measure the $\mathcal{B.R.}$ of the $B^0 \rightarrow D^0 \bar{D}^0 K^{*0}$. The way to perform this measurement is to refer the value to a reference channel. The master formula that one has to use to perform this measurement is ¹⁵:

$$\frac{N_{event}(B^0 \rightarrow D^0 \bar{D}^0 K^{*0})}{N_{event}(B^+ \rightarrow D^0 \bar{D}^0 K^+)} = \frac{\mathcal{L}}{\mathcal{L}} \times \frac{\sigma_{b\bar{b}}}{\sigma_{b\bar{b}}} \times \frac{2 \times f_{B^0}}{2 \times f_{B^+}} \times \frac{\mathcal{B.R.}(B^0 \rightarrow D^0 \bar{D}^0 K^{*0})}{\mathcal{B.R.}(B^+ \rightarrow D^0 \bar{D}^0 K^+)} \times \frac{\mathcal{B.R.}(D^0 \rightarrow K^- \pi^+)}{\mathcal{B.R.}(D^0 \rightarrow K^- \pi^+)} \times \frac{\mathcal{B.R.}(\bar{D}^0 \rightarrow K^+ \pi^-)}{\mathcal{B.R.}(\bar{D}^0 \rightarrow K^+ \pi^-)} \times \frac{\mathcal{B.R.}(K^{*0} \rightarrow K^- \pi^+)}{1} \times \frac{\epsilon_{tot}^*}{\epsilon_{tot}^{**}} \quad (1.1)$$

where

$$\epsilon_{tot} = \epsilon_{geometric} \times \epsilon_{trigger} \times \epsilon_{Selection} \quad (1.2)$$

After a pre-selection¹⁶ and using multivariate analysis (MVA) technique¹⁷ it has been possible to obtain a rather clean sample of B^+ mesons in the $B^+ \rightarrow D^0 \bar{D}^0 K^+$ as shown in fig 1.5.

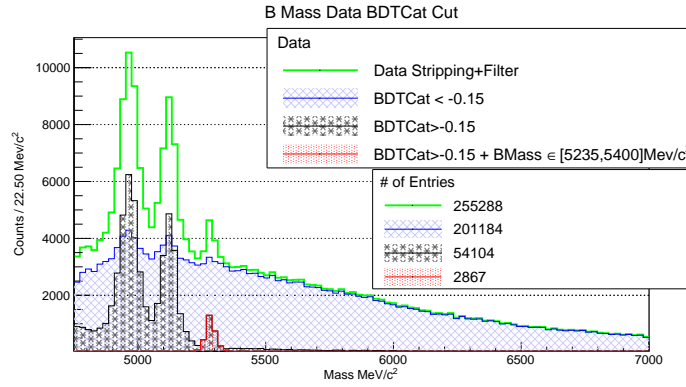


Figure 1.5: Reconstructed B mass spectrum for the 2011 and 2012 LHCb data in the $B^+ \rightarrow D^0 \bar{D}^0 K^+$ channel. Data Stripping + Filter are the pre-selected B candidates. The BDTCat is the MVA classifier which permits to separate background-like and signal-like candidates. The cut value set to -0.15 has been chosen maximising the $\frac{S}{\sqrt{S+B}}$ figure of merit (here ~ 40). The two peaks below the nominal B^+ mass consists into reconstructed D mesons from the strong $D^* \rightarrow D\pi$ decay where the π is outside the LHCb acceptance.

Using the sample of B candidates obtained, a very preliminary Dalitz study has been done looking to the 2- D plot made by the M_{A+B}^2 and M_{B+C}^2 invariant masses distributions, where A, B, C are the products of the 3-body decay $X \rightarrow ABC$ decay. The obtained distribution is shown in Fig 1.6.

1.5.3 PRELIMINARY RESULTS

The analysis is still on going and only a full amplitude analysis will tell if there are other structures in the $B^+ \rightarrow D^0 \bar{D}^0 K^+$ and in the $B^0 \rightarrow D^0 \bar{D}^0 K^{*0}$. The presented work already highlights the presence of resonant structure in the $D^0 \rightarrow \bar{D}^0$ spectrum compatible with the $\psi(3770)$ (should be also present in $B^0 \rightarrow D^0 \bar{D}^0 K^{*0}$) and also a peak structure in the $D^0 K^+$ invariant mass spectrum compatible with the $D^*(2700)^+$ (this should not appear in $B^0 \rightarrow D^0 \bar{D}^0 K^{*0}$). In addition, a very preliminary mass spectrum of the B^0 has been obtained (not shown here) with a roughly estimated yield of 300 events compatible with a predicted yield of ~ 100 events. This preliminary study and result have been also presented at the *TESchool2014*, a summer school in high energy physics in Ukraine last summer. Further details about this preliminary work and a complete description of the physics case can be found here [8]

¹⁴ There are several discrepancies between observed states and predicted one in the $X \rightarrow D^{(*)} D^{(*)}$ and the nature of some of the observed one is not clear and unambiguously defined yet.

¹⁵ Several factors factorize.

¹⁶ Based on the truth matched candidates in the Monte Carlo simulation

¹⁷ It relies in machine learning algorithms able to disentangle and classify a signal-like and background like sample knowing the values of a set of input variables.

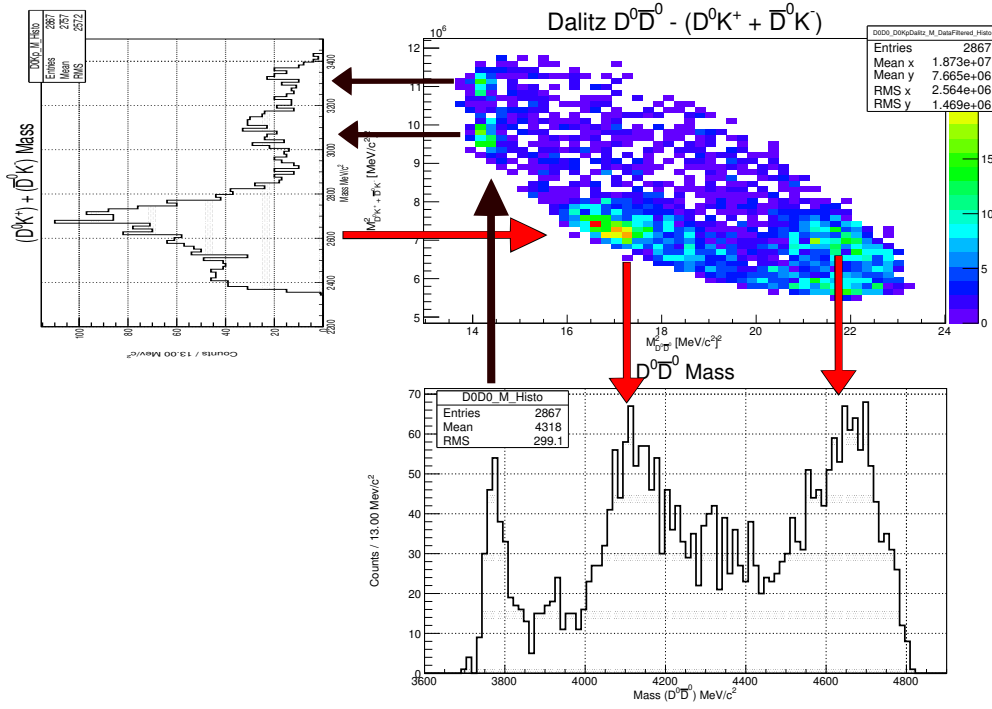


Figure 1.6: $B^+ \rightarrow D^0 \bar{D}^0 K^+$ Dalitz Plot of $(D^0 \bar{D}^0)$ vs. $(D^0 K^+ + c.c.)$. The accumulation of events on the top-left part are related to $B^+ \rightarrow \psi(3770) K^+ \rightarrow D^0 \bar{D}^0 K^+$ in fact the $\psi(3770)$ has a $J = 1$ and the corresponding typical pattern is the one that can be seen (two peaks). In addition another resonance is present in the central horizontal line and it correspond to a $J = 1$ resonance due to $D_{s1}^*(2700) \rightarrow D^0 K^\pm$.

2 CHOICE OF THESIS TOPIC

Explore the high energy regime of processes, understand the processes for which we live in a world dominated by matter instead of anti-matter and in general all the searches for physics beyond the standard model is for me as interesting and exciting as exploring the low energy regime of particle physics where *perturbation theory* (which is the theoretical framework for any kind of study of physics beyond the standard model) fails.

In that context, i think that understand the bridge connecting particle physics and nuclear physics (i.e. the *confinement* regime in QCD) is fundamental as well as exploring physics beyond the standard model, since for whatever good theory it's fundamental to have a precise description of what is happening in between two different regimes.

On top of that, a better knowledge of what happen in this low energy regime can also lead to better theoretical uncertainty estimation in almost all the analysis involig b and c hadrons, since from the knowledge and the understanding of the potential between confined quarks one can also infer and estimate for instance the *bag* parameters of heavy hadrons, as well as know with a better precision the effects of final state interactions and all the QCD corrections to apply in order to provide a precise theoretical prediction.

From this, it is easy to understand why i am interested in the study of exotic mesons and exotic structures rather than searching for physics beyond the standard model.

The large statistics of B hadrons produced at *LHCb* is infact an extraordinary laboratory to perform this studies and try to find new resonant states which are not "conventional". In addition, thanks to the branching ratio measurement in double charm decays one can also infer on the dynamic properties of b hadrons decay and investigate the final state interaction effects.

Such kind of channels (double charmed), even if they are not the *LHCb* priority, can also lead to very interesting discoveries and help at the same time the understanding of the QCD effective theories.

3 TIMETABLE FOR FUTURE

I am actually based at *LaL* and i expect to move in *Bristol University* in march 2016. Before that period, a public note regarding the new seeding algorithm will be produced and hopefully i will be able to perform the first task of my thesis, the *Branching Ratio* measurement for $B^0 \rightarrow D^0 \bar{D}^0 K^{*0}$. As described in that section, the selection is done with a *BDT* which is taking into account all the particles in the decay. This is something to avoid if one want to have a flat efficiency in the *Dalitz* plane. In addition to that the usage of *PID* variables in the *BDT* will complicate the analysis when the systematics errors will be calculated because that variables are not well modelled in the *MC*. In order to obtain similar efficiencies in the *Dalitz* plane for the interesting and the reference channel, the idea is to train and test a new *BDT* only for the D^0 selection without including the *PID* variables for their daughters using as signal-like sample the truth matched *MC* of the reference channel and as background like sample the sidebands of the D^0 in $B^+ \rightarrow D^0 \pi^+$ data sample. In such a way we will have the same *BDT* applied to the two D daughters and a third global one using as input output of the *BDT* classifier output of the D^0 ones and some topological and kinematical variables of the K^+ (K^*). In such a way we would expect

to obtain the same efficiencies in the *Dalitz* plane for the reference and the interest channel. This will be particularly important when the angular analysis will be performed in order to figure out the presence of some resonance in the *Dalitz* plane.

Regarding the tracking algorithm, i will also continue to work on that and try to improve it, but not full time involved as it has been untill now, and probably i will try to exploit the presence of additional bugs in the full simulation chain from time to time.

REFERENCES

- [1] LHCb Collaboration, *The LHCb Detector at the LHC*, JINST 3(2008) S08005
- [2] LHCb collaboration, *Letter of Intent for the LHCb Upgrade*, CERN-LHCC-2011-001, March 2011.
- [3] LHCb collaboration, *Framework TDR for the LHCb Upgrade*, CERN-LHCC-2012-007, May 2012.
- [4] LHCb collaboration, *LHCb Scintillating Fibre Tracker Technical Design Repoxrt*, CERN-LHCC-2014-001; LHCb TDR 15.
- [5] Renato Quagliani, *LaL internal presentation about the test beam*, <https://indico.lal.in2p3.fr/event/2506/contribution/1/material/slides/0.pdf>
- [6] Renato Quagliani, *Joint SciFi Tracker Simulation- Test Beam Meeting*, <https://indico.cern.ch/event/354578/contribution/5/material/slides/0.pdf>
- [7] Renato Quagliani, *Master Degree thesis*, <https://dbms.ilrt.bris.ac.uk/media/user/334129/tesi.pdf>